Elementary excitations in quantum Bose fluids: Application to liquid ^{4}He

M. Saarela
Department of Theoretical Physics, University of Oulu, Linnanmaa, SF-90570 Oulu, Finland
(Received 15 July 1985)

The optimizing Euler equations for the dynamic linear-response function are derived starting from the Jastrow ansatz for the wave function and including also the backflow effect. The elementary excitations in liquid ^{4}He are calculated consistently using the hypernetted-chain approximation for the uniform system as well as for weakly disturbed static and dynamic systems. The resulting excitation-energy spectrum is found to agree well with experiments up to the maxon region giving a maxon energy of 14.05 K and a roton energy of 11.7 K.

I. INTRODUCTION

For three decades the Bijl-Feynman dispersion relation[1,2]

$$\epsilon_k = \frac{\hbar^2 k^2}{2mS(k)} \tag{1}$$

has served as a starting point in discussions of the excitations in liquid ^{4}He. In the long-wavelength limit the relation becomes exact if the exact structure function $S(k)$ is used, whereas in the roton region it overestimates the excitation spectrum by a factor of 2. The backflow effect introduced by Feynman and Cohen[3] considerably improved the agreement with experiments, but still a deviation of some 50% in the roton energy remained. These works inspired a number of microscopic studies based on a Jastrow-type wave function[4] and perturbative corrections to it,[5–7] leading recently to good agreement with experiments.[7]

In this work we shall take a slightly different point of view in calculating the elementary excitations in quantum Bose systems, following the work by Ripka.[8] In order to describe nonequilibrium phenomena he assumed the wave function of the system to be of the Jastrow form, allowing for complex one- and two-particle correlation factors. Therefore,

$$\psi(\mathbf{r}_1,\ldots,\mathbf{r}_A;t) = \exp(\tfrac{1}{2}R + iI) \tag{2}$$

with

$$R = \sum_i u(\mathbf{r}_i;t) + \sum_{\substack{i,j\\(i<j)}} v(\mathbf{r}_i,\mathbf{r}_j;t)\ ,$$
$$I = \sum_i a(\mathbf{r}_i;t) + \sum_{\substack{i,j\\(i<j)}} b(\mathbf{r}_i,\mathbf{r}_j;t)\ . \tag{3}$$

The one-particle correlation function $u(\mathbf{r}_i;t)$ enters due to inhomogeneity of the system and currents present in the dynamic system necessitate a nonvanishing imaginary part. A direct derivation of the one- and two-particle currents[9] using the wave function of Eq. (2) leads to the expressions

$$\mathbf{j}^{(1)}(\mathbf{r}_1;t) = \frac{\hbar}{m}\left[\rho_1\nabla_1 a_1 + \int d^3r_2\rho_{12}^{(2)}\nabla_1 b_{12}\right] \tag{4}$$

and

$$\mathbf{j}_1^{(2)}(\mathbf{r}_1,\mathbf{r}_2;t) = \frac{\hbar}{m}\left[\rho_{12}^{(2)}(\nabla_1 a_1 + \nabla_1 b_{12}) + \int d^3r_3\rho_{123}^{(3)}\nabla_1 b_{13}\right]\ , \tag{5}$$

respectively. Here we have introduced the shorthand notations $f_1 = f(\mathbf{r}_1;t)$, $e_{12} = e(\mathbf{r}_1,\mathbf{r}_2;t)$ and employed the usual definitions for the densities,

$$\rho_1 = \frac{A}{\langle\psi|\psi\rangle}\int d\tau_1|\psi|^2\ ,$$
$$\rho_{12}^{(2)} = \frac{A(A-1)}{\langle\psi|\psi\rangle}\int d\tau_2|\psi|^2 = \rho_1\rho_2 g_{12}\ , \tag{6}$$
$$\rho_{123}^{(3)} = \frac{A(A-1)(A-2)}{\langle\psi|\psi\rangle}\int d\tau_3|\psi|^2 = \rho_1\rho_2\rho_3 g_{123}\ .$$

The last two equations relate the two- and three-particle densities into the corresponding distribution functions g_{12} and g_{123}. The integration over the second coordinate in Eq. (5) yields the sequential condition for the currents

$$\int d^3r_2[\mathbf{j}_1^{(2)}(\mathbf{r}_1,\mathbf{r}_2,t) - \rho_2\mathbf{j}^{(1)}(\mathbf{r}_1)] = -\mathbf{j}^{(1)}(\mathbf{r}_1)\ . \tag{7}$$

The elementary excitations should transport momentum and energy without an actual macroscopic transport of mass. This enforces the conservation equation for probability density which at the two-particle level can be written in the form

$$\frac{\partial}{\partial t}\rho_{12}^{(2)} + \nabla_1\cdot\mathbf{j}_1^{(2)}(\mathbf{r}_1,\mathbf{r}_2;t) + \nabla_2\cdot\mathbf{j}_2^{(2)}(\mathbf{r}_1,\mathbf{r}_2;t) = 0\ . \tag{8}$$

The use of the sequential condition (7) then gives the single-particle continuity equation

$$\frac{\partial}{\partial t}\rho_1 + \nabla_1\cdot\mathbf{j}^{(1)}(\mathbf{r}_1;t) = 0\ . \tag{9}$$

If the density ρ_1 and the radial distribution functions g_{12} and g_{123} were known we could solve for the currents from Eqs. (8) and (9) and then calculate the dynamic properties

 ©1986 The American Physical Society

of the system. In order to reach this goal we require that the integral[10]

$$\mathscr{A}[\Psi]=\int dt\frac{\langle\Psi(t)\,|\,H-i\hbar(\partial/\partial t)\,|\,\Psi(t)\rangle}{\langle\Psi(t)\,|\,\Psi(t)\rangle} \tag{10}$$

including the Hamiltonian H of the system is stationary against arbitrary variations of the wave function $\Psi(t)$,

$$\Psi(t)=e^{-iA\mu t/\hbar}\psi(t)\ . \tag{11}$$

The model wave function $\psi(t)$ is the Jastrow function (2) and μ is the chemical potential multiplied by the particle number A.

In this work we will solve this optimization problem within the hypernetted-chain (HNC) approximation analogously to the solution of the problem studied in Ref. 11. The resulting equations determine the properties of the dynamic inhomogeneous boson system. As an application, we study the case where a weak external disturbance $\delta U(k,\omega)$ with fixed momentum and frequency is applied to the uniform liquid ^{4}He. As a solution we obtain the dynamic linear-response function $\chi(k,\omega)$. The poles of $\chi(k,\omega)$, determine the dispersion relation of the elementary excitations in liquid ^{4}He which can be compared to measurements.

A similar approach was taken in a series of interesting papers by Krotscheck *et al.*[12] They investigated various properties of the free surface starting from a wave function where only the one-particle correlation function was allowed to be time dependent. This makes the numerical calculations tractable for strongly inhomogeneous systems like surfaces. In the limit of uniform ^{4}He the dispersion relation becomes the Bijl-Feynman relation of Eq. (1). The present work adds the important backflow effect within a scheme where the functional form of the backflow becomes optimized.

In Sec. II we derive the Euler-Lagrange equations for the dynamic boson system. In Sec. III the linear-response function $\chi(k,\omega)$ is evaluated and the elementary excitations obtained from the poles of $\chi(k,\omega)$ are determined and compared with experiments in Sec. IV.

II. OPTIMIZATION OF THE DYNAMIC SYSTEM

The Hamiltonian of the dynamic boson system,

$$H=-\frac{\hbar^2}{2m}\sum_{i=1}^{A}\nabla_i^2+\sum_{\substack{i,j\\(i<j)}}^{A}V(\,|\,\mathbf{r}_i-\mathbf{r}_j\,|\,)+\sum_{i=1}^{A}U_{\text{ext}}(\mathbf{r}_i;t)\ , \tag{12}$$

contains the two-particle potential $V(\,|\,\mathbf{r}_i-\mathbf{r}_j\,|\,)$ and a time-dependent, external, single-particle potential $U_{\text{ext}}(\mathbf{r}_i;t)$. Its expectation value

$$E(t)=\frac{\langle\Psi(t)\,|\,H\,|\,\Psi(t)\rangle}{\langle\Psi(t)\,|\,\Psi(t)\rangle} \tag{13}$$

with the wave function defined in Eq. (11) can be readily evaluated, yielding

$$E(t)=\int d^3r_1\left[\rho_1U_{\text{ext}}(\mathbf{r}_1;t)+\frac{\hbar^2}{2m}\{[\nabla_1(\rho_1)^{1/2}]^2+\rho_1(\nabla_1a_1)^2\}\right]$$
$$+\tfrac{1}{2}\int d^3r_1d^3r_2\rho_1\rho_2\left[H_{12}+\frac{\hbar^2}{m}g_{12}[(\nabla_1b_{12})^2+2\nabla_1a_1\cdot\nabla_1b_{12}]\right]+\frac{\hbar^2}{2m}\int d^3r_1d^3r_2d^3r_3\rho_1\rho_2\rho_3g_{123}\nabla_1b_{12}\cdot\nabla_1b_{13}\ . \tag{14}$$

The HNC approximation

$$g_{12}=e^{v_{12}+N_{12}} \tag{15}$$

determines the nodal sum N_{12} and the quantity H_{12} is defined as

$$H_{12}=V_{12}g_{12}+\frac{\hbar^2}{m}\{[\nabla_1(g_{12})^{1/2}]^2-\tfrac{1}{4}\nabla_1g_{12}\cdot\nabla_1N_{12}\}\ . \tag{16}$$

As the unperturbed reference system we take a uniform, time-independent fluid which is found by setting $\rho_1=\rho_2\equiv$const and $U_{\text{ext}}\equiv 0$. The imaginary parts, a_1 and b_{12}, of the wave function will then vanish. Such a system has energy E_0

$$\frac{E_0}{A}=\frac{\rho_0}{2}\int d^3r_{12}H_{12} \tag{17}$$

and pressure P

$$\frac{P}{\rho_0}=\frac{E_0}{A}-\frac{\hbar^2\rho_0}{8m}\int d^3r_{12}\nabla_1N_{12}\cdot\nabla_1C_{12}\ , \tag{18}$$

giving the chemical potential $\mu=(E_0/A)+(P/\rho_0)$. The direct correlation function C_{12} is defined by the relation

$$C_{12}=g_{12}-1-N_{12}\ . \tag{19}$$

Inserting the results of Eqs. (13) and (14) and working out the time derivative, we can write the variational problem of Eq. (10) in the form

$$\delta\int dt\left[E(t)-A\mu+\hbar\left[\int d^3r_1\rho_1\dot{a}_1+\tfrac{1}{2}\int d^3r_1d^3r_2\rho_1\rho_2g_{12}\dot{b}_{12}\right]\right]=0\ , \tag{20}$$

where the overdots represent the time derivatives. Equation (20) contains four independent functions which are chosen to be $(\rho_1)^{1/2}$, $(g_{12})^{1/2}$, a_1, and b_{12}. The nodal sum depends on the above quantities through the Ornstein-Zernike relation

$$N_{12}=\int d^3r_3\rho_3(g_{13}-1)C_{32}\ . \tag{21}$$

Furthermore the three-particle distribution function g_{123} is approximated by the convolution approximation.[9] A straightforward variation[11] of Eq. (20) gives four coupled Euler-Lagrange equations

$$\begin{aligned}
&-\frac{\hbar^2}{2m}\nabla_1^2(\rho_1)^{1/2}+(\rho_1)^{1/2}[W_\rho(1)+U_{\text{ext}}(1)+F_\rho(1)]=\mu(\rho_1)^{1/2}\ ,\\
&-\frac{\hbar^2}{m}\nabla_1\cdot[\rho_1\nabla_1(g_{12})^{1/2}]+(g_{12})^{1/2}[\rho_1V_{12}+W_g(1,2)+F_g(1,2)]+(1\leftrightarrow 2)=0\ ,\\
&\nabla_1\cdot\mathbf{j}^{(1)}(1)+\dot{\rho}_1=0\ ,\\
&\nabla_1\cdot\mathbf{j}_1^{(2)}(1,2)+\nabla_2\cdot\mathbf{j}_2^{(2)}(1,2)+\dot{\rho}_{12}^{(2)}=0\ ,
\end{aligned} \tag{22}$$

with the induced potentials

$$W_\rho(1)=\tfrac{1}{2}\int d^3r_2\rho_2\left[H_{12}+H_{21}-\frac{\hbar^2}{4m}\nabla_2N_{12}\cdot\nabla_2C_{21}\right]\ , \tag{23}$$

$$W_g(1,2)=\frac{\hbar^2}{2m}\nabla_1\cdot(\rho_1\nabla_1N_{12})-\frac{\hbar^2\rho_1}{4m}\int d^3r_3\rho_3\nabla_3C_{13}\cdot\nabla_3C_{32}\ ,$$

and

$$\begin{aligned}
F_\rho(1)&=\hbar\left[\dot{a}_1+\int d^3r_2\rho_2g_{12}\dot{b}_{12}\right]+O(a_1^2,b_{12}^2)\ ,\\
F_g(1,2)&=\hbar\rho_1\dot{b}_{12}+O(a_1^2,b_{12}^2)\ .
\end{aligned} \tag{24}$$

The first two Euler equations are familiar from the variation of the static system but include additional terms due to the imaginary part of the wave function (2) defined in Eqs. (24). In the calculation of the response function we are interested only in the terms linear in a_1 and b_{12} and, thus, the quadratic ones will drop out. The last two equations are just the continuity equations, (9) and (8), with the currents defined in Eqs. (4) and (5). These four Euler equations describe the properties of an inhomogeneous time-dependent boson system under an external driving potential $U_{\text{ext}}(\mathbf{r}_1,t)$ as long as the Jastrow ansatz and the HNC approximation are valid. They are of course very complicated to solve for strongly inhomogeneous systems but for small deviations from uniformity we can linearize the equations and find the solution for the linear-response function.

III. THE DYNAMIC LINEAR-RESPONSE FUNCTION

In order to calculate the dynamic linear-response function $\chi(k,\omega)$ we take the single-particle potential in the Hamiltonian (12) to be a weak external disturbance with momentum k and frequency ω, $U_{\text{ext}}(\mathbf{r}_1,t)\rightarrow\delta U(k,\omega)$. It disturbs the uniform boson system, e.g., liquid ^{4}He, and the response of the system must satisfy the Euler equations (22). Since we are interested only in the linear response we shall expand the Euler equations in terms of small changes in the density ρ_0 and the distribution function g_{12}^0, $\rho_1=\rho_0(1+\xi_1)$, and $g_{12}=g_{12}^0(1+h_{12})$, respectively. From the expansion we keep only the terms linear in ξ_1 and h_{12} as well as terms linear in a_1 and b_{12}.

It is more natural to work in the Fourier space and we choose the transformations

$$\begin{aligned}
\xi_1&=\xi(\mathbf{r}_1;t)=\int\frac{d\omega d^3k}{(2\pi)^4\rho_0}e^{i(\mathbf{k}\cdot\mathbf{r}_1+\omega t)}\xi_{k,\omega}\ ,\\
h_{12}&=h(\mathbf{r}_1,\mathbf{r}_2;t)\\
&=\int\frac{d\omega\, d^3q\, d^3k}{(2\pi)^7\rho_0^2}e^{i[\mathbf{k}\cdot\mathbf{r}_1+\mathbf{q}\cdot(\mathbf{r}_1-\mathbf{r}_2)+\omega t]}h_{k,\omega}(\mathbf{q})\ .
\end{aligned} \tag{25}$$

Similar transformations apply for a_1 and b_{12}.

The response function

$$\chi(k,\omega)\equiv\rho_0\xi_{k,\omega}/\delta U(k,\omega) \tag{26}$$

is readily obtained from the first Euler equation,

$$\rho_0\chi^{-1}(k,\omega)=-\frac{\hbar^2k^2}{4m}-\frac{1}{\xi_{k,\omega}}\mathcal{F}[\delta W_\rho(1)+F_\rho(1)]\ , \tag{27}$$

where the notation $\mathcal{F}[\ ]$ means the Fourier transform of the quantities in square brackets and $\delta W_\rho(1)$ is a small change in the induced potential $W_\rho(1)$. [As pointed out earlier, $F_\rho(1)$ is already linear in a_1 and b_{12}.]

Detailed evaluation of $\mathcal{F}[\delta W_\rho(1)]$ is done in Ref. 11 and we write it here in the form

$$\frac{1}{\xi_{k,\omega}}\mathcal{F}[\delta W_\rho(1)]=\frac{\hbar^2}{4m}\left[\frac{k^2}{S_k^2}(1-S_k^2)+W_{k,\omega}\right]\ , \tag{28}$$

where $S_k\equiv S(|\mathbf{k}|)$ is the structure function of the uniform system. The expression for $W_{k,\omega}$ is rather lengthy and given in the Appendix. The Fourier transform $\mathcal{F}[F_\rho(1)]$ can be directly obtained from the solution of the continuity equations (8) and (9). Therefore,

$$\mathcal{F}[F_\rho(1)]=-\frac{m\omega^2}{k^2}(1+M_{k,\omega}) \tag{29}$$

with

$$M_{k,\omega}=\int \frac{d^3q}{(2\pi)^3\rho_0}\mathbf{k}\cdot\mathbf{q}(S_q-1)B_{k,\omega}(\mathbf{q}) , \tag{30}$$

where

$$B_{k,\omega}(\mathbf{q})=-\frac{i\hbar}{m\omega\xi_{k,\omega}}\mathscr{F}[b_{12}] . \tag{31}$$

Inserting the results (28) and (29) into Eq. (27) we find that

$$\rho_0\chi^{-1}(k,\omega)=-\frac{\hbar^2}{4m}\left[\frac{k^2}{S_k^2}+W_{k,\omega}\right]+\frac{m\omega^2}{k^2}(1+M_{k,\omega}) . \tag{32}$$

When $\omega=0$ we recover from Eq. (32) the static linear-response function[11]

$$\rho_0\chi^{-1}(k)=-\frac{\hbar^2}{4m}\left[\frac{k^2}{S_k^2}+W_{k,\omega=0}\right] , \tag{33}$$

which in the limit of $k=0$ in liquid ^{4}He becomes

$$\lim_{k\to 0}\rho_0\chi^{-1}(k)=-\frac{1}{\rho_0 K}=-mc^2 , \tag{34}$$

where K is the thermodynamic compressibility and c the speed of sound.

The poles of the response function, $\chi^{-1}(k,\omega)=0$, determine the dispersion relation $\omega=\omega(k)$ and hence the excitation spectrum $\epsilon_k=\hbar\omega$ in boson fluids. It can be calculated iteratively since the quantities $W_{k,\omega}$ and $M_{k,\omega}$ are only weakly dependent on ω. The expression for ϵ_k can then be written in the form[13]

$$\epsilon_k=\frac{\hbar^2k^2}{2m_k^*S_k} , \tag{35}$$

where

$$m_k^*=m(1+M_{k,\epsilon_k})^{1/2}\left[1+\frac{S_k^2}{k^2}W_{k,\epsilon_k}\right]^{-1/2} .$$

In the long-wavelength limit $\lim_{k\to 0}M_{k,\omega=0}=0$ [see Eq. (30) and the Appendix] and $\lim_{k\to 0}W_{k,\omega=0}=\text{const.}$[11] Thus we find from Eqs. (33)–(35) the familiar linear behavior of the excitations

$$\lim_{k\to 0}\epsilon_k=\hbar ck . \tag{36}$$

We should point out here that the speed of sound calculated from the slope of S_k at small k, when the uniform ^{4}He system is solved, within the HNC approximation at zero pressure, does not agree with the one of Eq. (34). This is due to the fact that $\lim_{k\to 0}W_{k,\omega=0}\neq 0$.

In order to find agreement between these two ways of calculating the speed of sound one should add the elementary diagrams and the three-body correlations to the HNC approximation. It is known (see, i.e., Refs. 14 and 15) that they improve the agreement with the experimental saturation energy and density in liquid ^{4}He and also give the correct behavior for the slope of the static structure function at $k\approx 0$. This means that the function $W_{k,\omega}$ appearing in both of the expressions for the static linear-response function, Eq. (33), and the excitation spectrum, Eq. (35), becomes small compared to k^2/S_k^2 at $k\approx 0$. However, since our aim in this work is to discuss the effect of the optimized complex one- and two-body correlations to the elementary excitations we shall leave a more quantitative study of the elementary diagrams and the three-body correlations to the future.

In the case of the charged boson gas, where the small-k behavior of the structure function is quadratic,

$$\lim_{k\to 0}S_k=\frac{\hbar k^2}{2m\omega_p} , \tag{37}$$

and inverse to the plasma frequency ω_p, the elementary excitations of Eq. (35) will start from a constant

$$\lim_{k\to 0}\epsilon_k=\hbar\omega_p , \tag{38}$$

because $\lim_{k\to 0}W_{k,\omega=0}=\text{const}$ (see Ref. 11).

In order to calculate the full excitation curve and especially to study its behavior in the roton region in ^{4}He, we must solve the last three Euler equations in (22). The easiest one is the one-particle continuity equation which in momentum space can be written in the form

$$k^2A_{k,\omega}=1-\int \frac{d^3q}{(2\pi)^3\rho_0}(S_q-1)\mathbf{k}\cdot(\mathbf{k}+\mathbf{q}) \times B_{k,\omega}(\mathbf{q})-k^2B_{k,\omega}(0) \tag{39}$$

with

$$A_{k,\omega}=-\frac{i\hbar}{m\omega\xi_{k,\omega}}\mathscr{F}[a_1] .$$

The two-particle equations in (22) lead to integral equations

$$h_{k,\omega}(\mathbf{q})-\int \frac{d^3q'}{(2\pi)^3\rho_0}h_{k,\omega}(\mathbf{q}')K_k(\mathbf{q},\mathbf{q}') =T_k(\mathbf{q})+\omega^2t_k(\mathbf{q})B_{k,\omega}(\mathbf{q}) , \tag{40}$$

$$B_{k,\omega}(\mathbf{q})+\int \frac{d^3q'}{(2\pi)^3\rho_0}B_{k,\omega}(\mathbf{q}')\overline{K}_k(\mathbf{q},\mathbf{q}') =\overline{T}_k(\mathbf{q})+\overline{t}_k(\mathbf{q})G_{k,\omega}(\mathbf{q}) \tag{41}$$

with

$$G_{k,\omega}(\mathbf{q})=h_{k,\omega}(\mathbf{q})+\int \frac{d^3q'}{(2\pi)^3\rho_0}h_{k,\omega}(\mathbf{q}')(S_{q-q'}-1) , \tag{42}$$

where

$$G_{q,\omega}(\mathbf{q})=\mathscr{F}[\delta g_{12}]/\xi_{k,\omega}$$

and

$$h_{k,\omega}(\mathbf{q})=\mathscr{F}\left[\frac{\delta g_{12}}{g_{12}^0}\right]\Big/\xi_{k,\omega} .$$

The expressions for quantities $K_k(\mathbf{q},\mathbf{q}')$, $\overline{K}_k(\mathbf{q},\mathbf{q}')$, $T_k(\mathbf{q})$, $\overline{T}_k(\mathbf{q})$, $t_k(\mathbf{q})$, and $\overline{t}_k(\mathbf{q})$ are given in the Appendix. They are all independent of the frequency ω and contain only ground-state quantities such as the structure function and

the logarithm of the radial distribution function. The frequency dependence enters through the second term on the right-hand side of Eq. (40), $\omega^2 t_k(\mathbf{q}) B_{k,\omega}(\mathbf{q})$.

The two coupled integral equations (40) and (41) are rather complicated to solve numerically because the functions $h_{k,\omega}(\mathbf{q})$ and $B_{k,\omega}(\mathbf{q})$ contain two variables $|\mathbf{q}|$ and the angle $\theta_{k,q}$ between vectors $\mathbf{k}$ and $\mathbf{q}$. By expanding these functions in terms of Legendre polynomials and performing the angular integrations analytically we obtain a set of coupled equations for the multipliers of the expansion with single variable $|\mathbf{q}|$. (The frequency ω and momentum k are merely parameters.) In the expansion we include polynomials up to $l=6$.

IV. THE ENERGY SPECTRUM OF LIQUID ^{4}He

The Jastrow ansatz for the wave function together with the HNC approximation lead to the set of Euler equations (22) and provide us with a well-defined scheme, where the uniform boson system as well as the weakly disturbed static and dynamic systems can be solved within the same set of equations. The input to these equations is the two-particle potential which in the case of liquid ^{4}He is chosen to be the Aziz potential.[16]

The experiments we would like to describe here are the excitation spectrum measurements done at saturated vapor pressure (SVP).[17,18] For that purpose we must first solve the uniform system and find its saturation density which with the Aziz potential is $\rho_0=0.0175$ Å^{-3}. The structure function obtained from these calculations has too shallow a peak and it is too steep in the long-wavelength limit as shown in Fig. 1. By including elementary diagrams and three-particle correlations a good agreement with experiments is found.[15]

The next test of our equations is the static linear-response function[11] $\chi(k)$, which is shown together with experimental results in Fig. 2. The agreement is very

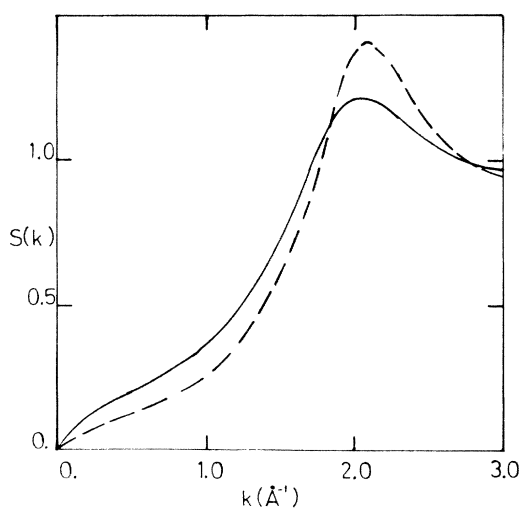

FIG. 1. Structure function of liquid ^{4}He using the Aziz potential (Ref. 16). The solid curve is the optimized Jastrow-HNC result evaluated the SVP corresponding to the density $\rho_0=0.0175$ Å^{-3}. The dashed curve is the triplet-Feenberg result of Ref. 15 which compares well with experiments.

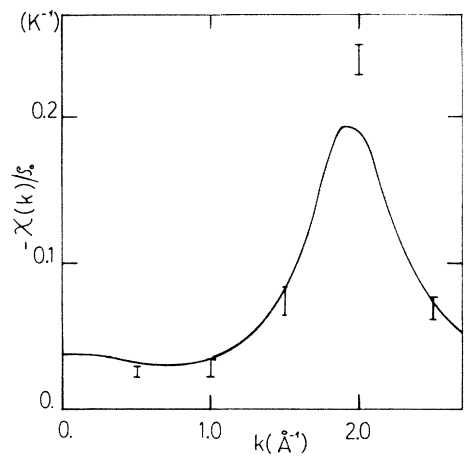

FIG. 2. Static linear-response function of liquid ^{4}He at SVP compared with the measured results of Ref. 18.

good for small and large momenta. The speed of sound found from Eq. (34) is $c \approx 236$ m/s, whereas experiments give $c_{\text{expt}}=237$ m/s,[17] but the peak of $\chi(k)$ is not high enough.

The excitation energy spectrum of Eq. (35) is calculated through iterations. We start by solving Eq. (40) when $\omega=0$. This gives us the static $h_{k,\omega=0}(\mathbf{q})$, which can be used to calculate $B_{k,0}(q)$ from Eqs. (42) and (41) and then the quantities $M_{k,0}$ of Eq. (30) and $W_{k,0}$ of Eq. (A1). Inserting these into Eq. (35) we get the first approximation for ϵ_k. The next iteration is obtained by setting $\omega=\epsilon_k/\hbar$ and using in Eq. (40) the function $B_{k,\omega}(\mathbf{q})$ from the previous iteration step. It turns out that the ω dependence of ϵ_k is quite weak (less than 10%) and, thus, the iteration converges rapidly. There arises, however, one difficulty which is seen by inserting Eqs. (42) and (40) into Eq. (41). The factor multiplying $B_{k,\omega}(\mathbf{q})$ is then $1-\omega^2 t(\mathbf{q})\bar{t}(\mathbf{q})$. Because the integral term in (41) is small compared to unity we must require that $\omega^2 t(\mathbf{q})\bar{t}(\mathbf{q})<1$ at all values of $\mathbf{q}$ which leads to the condition

$$\hbar\omega \lesssim \frac{\hbar^2 k^2}{4mS_{k/2}} . \tag{43}$$

If this condition is violated during the iterations, the Legendre expansion of Eqs. (41) and (40) will not converge any more. The reason for this difficulty is not well understood, but if our system were consistent with the fluctuation dissipation theorem

$$S_k=\int_0^\infty \frac{d\omega}{2\pi}\frac{2\hbar}{\rho_0}\mathrm{Im}\chi(k,\omega) \tag{44}$$

leading in the one-pole approximation for $\chi(k,\omega)$ in Eq. (32) to the energy spectrum

$$\epsilon_k=\frac{\hbar^2 k^2}{2mS_k(1+M_{k,\epsilon_k})} , \tag{45}$$

then this difficulty would not occur.

In Fig. 3 we plot the calculated excitation spectrum. It follows the experimental points well up to $k\sim 1.5$ Å^{-1}, giving a maxon energy 14.05 K compared to the experimental one of 13.8 K. The linear behavior at small k is

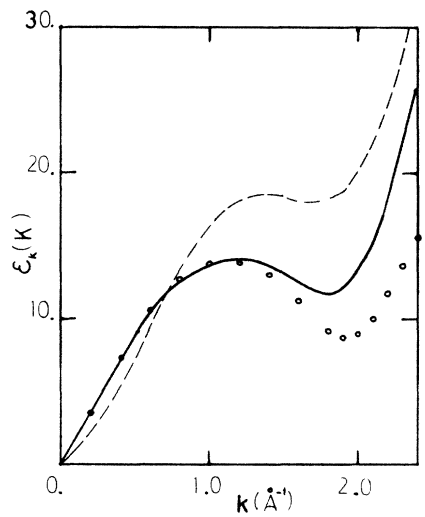

FIG. 3. Elementary excitation spectrum of liquid ^{4}He. The solid curve is the result of the present work the dashed curve is the Bijl-Feynman dispersion relation using the structure function of Fig. 1 and the open circles are the measurements of Ref. 18.

determined by the speed of sound [see Eq. (36)], which agrees with experiments within 1%. In order to avoid violation of the condition (43) when $k<1$ Å^{-1}, we have evaluated the functions $M_{k,\omega}$ and $W_{k,\omega}$ needed for ϵ_k in Eq. (35) at $\omega=\hbar k^2/4mS_{k/2}$. As mentioned earlier, ϵ_k depends only weakly on ω during iterations and thus we believe that the present results are reliable.

In the roton region the calculated energies are clearly above the experiments. We found the roton energy 11.7 K compared to the experimental 8.7 K. Also the momentum at the minimum is slightly shifted towards smaller values of momenta. This is the deficiency of the HNC approximation in giving high enough peaks for the structure function and the static response function when $k\sim 2$ Å^{-1}.

For comparison, we also plot in Fig. 3 the optimized HNC result for the Bijl-Feynman relation of Eq. (1) calculated at the saturation density $\rho_0=0.0175$ Å^{-3}. It turns out to be quite a poor approximation both at small k and in the roton region.

Finally the function $M_{k,\omega}$ appearing in both of the energy expressions (35) and (45) is plotted in Fig. 4. It starts like k^2 when k is small and has a maximum in the maxon region.

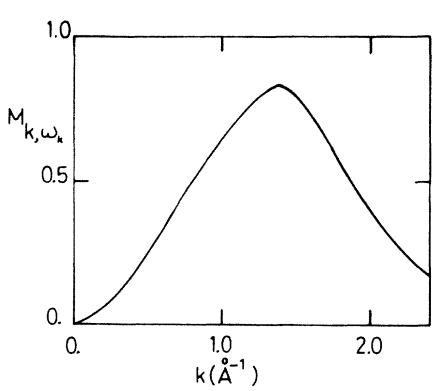

FIG. 4. Function $M_{k,\omega}$ defined in Eq. (30).

V. SUMMARY

We have derived the optimizing Euler equations for the dynamic inhomogeneous boson system starting from the Jastrow ansatz for the wave function which also includes the backflow factor. This set of four equations is solved when a weak external disturbance is applied to liquid ^{4}He. As a result, we get the dynamic linear-response function and the elementary excitation spectrum. Working consistently within the HNC approximation we find that the calculated energy spectrum agrees surprisingly well with experiments up to $k\sim 1.5$ Å^{-1}. The roton dip at $k\sim 1.85$ Å^{-1}, however, is not deep enough. This difficulty may be traced back to the too shallow peak in the structure function.

ACKNOWLEDGMENTS

The author would like to thank Professor A. Kallio, L. Lantto, P. Pietiläinen, and M. Puoskari for many valuable discussions.

APPENDIX

In this appendix we collect the lengthy formulas used in the calculation of the dynamic response function of a quantum Bose system. In order to profit from the symmetry of the functions $g_{12}=g_{21}$ and $b_{12}=b_{21}$ we change the momentum space variable $\mathbf{q}\to\mathbf{q}-(\mathbf{k}/2)$ in the evaluation of these two-particle functions from the integral equations (40)–(42). The functions $h_{k,\omega}(\mathbf{q})$, $G_{k,\omega}(\mathbf{q})$, and $B_{k,\omega}(\mathbf{q})$ are then symmetric under the change of sign of the variable $\mathbf{q}$ and thus only even values of l are needed in the Legendre expansion. In the numerical calculations we take the maximum $l_{\max}=6$.

The expression for the quantity $W_{k,\omega}$ appearing in Eq. (28) may be written in terms of two integrals

$$W_{k,\omega}=\tfrac{1}{2}\int\frac{d^3q}{(2\pi)^3\rho_0}[I_k(\mathbf{q})+J_{k,\omega}(\mathbf{q})]\ , \tag{A1}$$

where

$$I_k(\mathbf{q})=R_k(\mathbf{q})Z_k(\mathbf{q})/X_k(\mathbf{q})+Y_k(\mathbf{q}) \tag{A2}$$

with

$$R_k(\mathbf{q})=\mathbf{k}\cdot\mathbf{q}(C_+C_--1)(S_+-S_-)-\tfrac{1}{2}k^2(S_+S_--1)$$
$$-(q^2+\tfrac{1}{4}k^2)C_+C_-(S_+S_-+S_++S_-)\ , \tag{A3}$$

$$Z_k(\mathbf{q})=\mathbf{k}\cdot(\tfrac{1}{2}\mathbf{k}+\mathbf{q})u_++\mathbf{k}\cdot(\tfrac{1}{2}\mathbf{k}-\mathbf{q})$$
$$\times u_-+(q^2-\tfrac{1}{4}k^2)C_+C_-\ , \tag{A4}$$

$$X_k(\mathbf{q})=\frac{(\frac{1}{2}\mathbf{k}+\mathbf{q})^2}{S_+}+\frac{(\frac{1}{2}\mathbf{k}-\mathbf{q})^2}{S_-}\ , \tag{A5}$$

$$Y_k(\mathbf{q})+C_+C_-[\mathbf{k}\cdot\mathbf{q}(S_+-S_-)+(q^2-\tfrac{1}{4}k^2)(S_+-1)(S_--1)+\tfrac{1}{2}k^2(2S_+S_--S_+-S_-)] , \quad (A6)$$

and

$$u_q \equiv \mathscr{F}[\ln g_{12}^0 - N_{12}] \equiv l_q - N_q . \quad (A7)$$

In the above formulas we have used the notation

$$f_\pm = f(|\tfrac{1}{2}\mathbf{k}\pm\mathbf{q}|) . \quad (A8)$$

The second term in the integral (A1) depends on the function $h_{k,\omega}(\mathbf{q})$ and thus also on ω

$$J_{k,\omega}(\mathbf{q}) = \int \frac{d^3q'}{(2\pi)^3\rho_0} h_{k,\omega}(\mathbf{q}') \times [U_k(\mathbf{q},\mathbf{q}')R_k(\mathbf{q})/X_k(\mathbf{q}) - L_k(\mathbf{q},\mathbf{q}')] \quad (A9)$$

with

$$U_k(\mathbf{q},\mathbf{q}') = 2(q^2+\tfrac{1}{4}k^2)(S_{q-q'}-1) - 2\mathbf{q}'\cdot(\mathbf{q}-\mathbf{q}')l_{q-q'} , \quad (A10)$$

$$L_k(\mathbf{q},\mathbf{q}') = [\mathbf{k}\cdot\mathbf{q}(S_+-S_-) + \tfrac{1}{2}k^2(S_++S_--2)](S_{q-q'}-1) . \quad (A11)$$

The integral equation (40) for $h_{k,\omega}(\mathbf{q})$,

$$h_{k,\omega}(\mathbf{q}) - \int \frac{d^3q'}{(2\pi)^3\rho_0} h_{k,\omega}(\mathbf{q}')K_k(\mathbf{q},\mathbf{q}') = T_k(\mathbf{q}) + \omega^2 t_k(\mathbf{q})B_{k,\omega}(\mathbf{q}) , \quad (A12)$$

includes the quantities

$$K_k(\mathbf{q},\mathbf{q}') = S_+S_-U_k(\mathbf{q},\mathbf{q}')/X_k(\mathbf{q}) - (S_{q-q'}-1) , \quad (A13)$$

$$T_k(\mathbf{q}) = S_+S_-Z_k(\mathbf{q})/X_k(\mathbf{q}) + (S_+-1)(S_--1) ,$$

and

$$t_k(\mathbf{q}) = \frac{4m^2}{\hbar^2} S_+S_-/X_k(\mathbf{q}) .$$

The integral equation (41) for $B_{k,\omega}(\mathbf{q})$ is obtained after the convolution approximation is used for q_{123}

$$B_{k,\omega}(\mathbf{q}) + \int \frac{d^3q'}{(2\pi)^3\rho_0} B_{k,\omega}(\mathbf{q}')\bar{K}_k(\mathbf{q},\mathbf{q}') = \bar{T}_k(\mathbf{q}) + \bar{t}_k(\mathbf{q})G_{k,\omega}(\mathbf{q}) . \quad (A14)$$

It contains the quantities

$$\bar{K}_k(\mathbf{q},\mathbf{q}') = \left[\frac{(\frac{1}{2}\mathbf{k}+\mathbf{q})\cdot(\frac{1}{2}\mathbf{k}+\mathbf{q}')}{S_+S'_+} + \frac{(\frac{1}{2}\mathbf{k}-\mathbf{q})\cdot(\frac{1}{2}\mathbf{k}-\mathbf{q}')}{S_-S'_-} \right] \times \frac{S'_+S'_-}{X_k(\mathbf{q})}(S_{q-q'}-1) ,$$

$$\bar{T}_k(\mathbf{q}) = \left[\frac{\mathbf{k}\cdot\mathbf{q}}{k^2}(S_+-S_-) + \tfrac{1}{2}(S_++S_--2) \right] \bar{t}_k(\mathbf{q}) , \quad (A15)$$

and

$$\bar{t}_k(\mathbf{q}) = \frac{1}{S_+S_-X_k(\mathbf{q})} .$$

Here we have used a notation $S'_\pm = S(|\tfrac{1}{2}\mathbf{k}\pm\mathbf{q}'|)$.

In the numerical calculations it is important to be careful with the singularity in $\bar{T}_k(\mathbf{q})$

$$\lim_{\mathbf{q}\to-\mathbf{k}/2} \bar{T}_k(\mathbf{q}) = \frac{S_k-1}{k^2} \lim_{\mathbf{q}\to\mathbf{k}/2} \frac{1}{S(|\frac{1}{2}\mathbf{k}-\mathbf{q}|)} , \quad (A16)$$

because only if $G_{k,\omega}(\mathbf{q})$ exactly fulfills Eqs. (42) and (40) at $\mathbf{q}=\mathbf{k}/2$, or, equivalently, the sequential condition[11]

$$\lim_{\mathbf{q}\to\mathbf{k}/2} G_{k,\omega}(\mathbf{q}) = 1 - S_k ,$$

then the singularity is canceled by the last term in Eq. (A14). This can be guaranteed by replacing $G_{k,\omega}(\mathbf{q})$ by its "solution" in terms of the integrals appearing in Eqs. (40) and (42) and then

$$\lim_{\mathbf{q}\to\mathbf{k}/2} T_k(\mathbf{q}) = 1 - S_k \quad (A17)$$

cancels the singularity.

One simplifying approximation is made in the calculation of the integral equation (A14) by substituting the term $S_{q-q'}-1$ in $\bar{K}_k(\mathbf{q},\mathbf{q}')$ by its angle average. This is unimportant for the numerical results but simplifies the Legendre expansion of the integral considerably.

[1]A. Bijl, Physica **7**, 869 (1940).
[2]R. P. Feynman, Phys. Rev. **94**, 262 (1954).
[3]R. P. Feynman and M. Cohen, Phys. Rev. **102**, 1189 (1956).
[4]T. C. Padmore and C. V. Chester, Phys. Rev. A **9**, 1725 (1974).
[5]D. K. Lee and F. J. Lee, Phys. Rev. B **11**, 4318 (1975).
[6]C. C. Chang and C. E. Cambell, Phys. Rev. B **13**, 3779 (1976); C. E. Cambell and F. J. Pinski, Nucl. Phys. A **328**, 210 (1979).
[7]K. E. Schmidt and V. R. Pandharipande, Phys. Rev. B **21**, 3945 (1980); E. Manousakis and V. R. Pandharipande, *ibid.* **30**, 5062 (1984).
[8]G. Ripka, Phys. Rep. **56**, 1 (1979).
[9]E. Feenberg, *Theory of Quantum Fluids* (Academic, New York 1969).
[10]See, for instance, D. J. Thouless, *The Quantum Mechanics of Many-Body Systems* (Academic, New York, 1961).
[11]M. Saarela, P. Pieteiläinen, and A. Kallio, Phys. Rev. B **27**, 231 (1983); M. Saarela, *ibid.* **29**, 191 (1984); **30**, 2925 (1984).
[12]E. Krotscheck, G.-X. Qian, and W. Kohn, Phys. Rev. B **31**, 4245 (1985); E. Krotscheck, *ibid.* **31**, 4258 (1985); **31**, 4267

(1985).

[13]A similar formula for ϵ_k was recently phenomenologically analyzed by A. Kallio, M. Puoskari, L. Lantto, and P. Pietiläinen, in *Proceedings of the Recent Progress in Many-Body Theories,* edited by H. Kümmel and M. L. Ristig (Springer-Verlag, Berlin, 1983), p. 210.

[14]R. A. Smith, A. Kallio, M. Puoskari, and P. Toropainen, Nucl. Phys. A **328**, 186 (1979).

[15]L. R. Whitney, F. J. Pinski, and C. E. Cambell, J. Low Temp. Phys. **44**, 367 (1981).

[16]R. A. Aziz, W. P. S. Nain, J. S. Carley, W. L. Taylor, and G. T. McConville, J. Chem. Phys. **70**, 4330 (1979).

[17]D. G. Henshaw and A. D. B. Woods, Phys. Rev. **121**, 1266 (1961).

[18]R. A. Cowley and A. D. B. Woods, Can. J. Phys. **49**, 177 (1971).